DOI: 10.2352/ISSN.2470-1173.2016.15.IPAS-024

OPTIMAL TRANSPARENT WAVELENGTH AND ARRANGEMENT FOR MULTISPECTRAL FILTER ARRAY

Yudai Yanagi†, Kazuma Shinoda†, Madoka Hasegawa† and Shigeo Kato†
Masahiro Ishikawa‡, Hideki Komagata‡, Naoki Kobayashi‡
†Graduate School of Engineering, Utsunomiya University, 7-1-2 Yoto, Utsunomiya, Tochigi, 321-8585 Japan
‡Faculty of Health and Medical Care, Saitama Medical University, 1397-1 Yamane, Hidaka, Saitama, 350-1241 Japan

Abstract

A single-camera one-shot multispectral imaging system with multispectral filter array (MSFA) has the potential to promote fast and low-cost multispectral imaging. Because the restoration accuracy of the image acquired with this imaging system depends on MSFA, optimization for MSFA has been demanded. Conventional optimizing methods have designed the versatile MSFA without dependence on the imaging object. In the field that requires multispectral images, an imaging object is often determined before designing MSFA. If MSFA can be designed based on the imaging object, the restoration accuracy becomes higher than the versatile MSFA of the conventional methods. In this paper, we propose an optimizing method for MSFA that uses the training data of the imaging object. The proposed method optimizes the observation wavelength and filter arrangement based on simulated annealing. The experiment results demonstrate that the proposed method outperforms conventional methods quantitatively.

1. Introduction

Multispectral images (MSIs) have been used in fields that require high-fidelity color reproductions, such as for medical applications and sugar content prediction. Various multispectral imaging systems have been proposed [1]-[7]. Among these systems, a single-camera one-shot multispectral imaging system with multispectral filter array (MSFA) has the potential to promote fast and low-cost multispectral imaging.

Figure 1 shows the MSI imaging system flow using MSFA. In this imaging system, the mosaicked image observed through MSFA needs to be interpolated in order to acquire a full-resolution multispectral image. The restoration accuracy of the interpolated MSI depends not only on the interpolation method, but also on MSFA. Recently, various interpolation methods for MSI have been proposed [1], [5], [7]. On the other hand, the method for designing MSFAs has not been studied sufficiently. Therefore, we focus on the design of MSFA in order to improve restoration accuracy.

Design methods for MSFA have been proposed [6]-[9]. The design of MSFA that improves restoration accuracy needs to consider spectral sensitivities and filter arrangement. Because restoration accuracy depends on the spectral sensitivities and filter arrangement of MSFA, optimization methods for spectral sensitivities or filter arrangement have been proposed [8]-[9]. Monno et al.'s method [8] improves restoration accuracy by optimizing the spectral sensitivity of five-band MSFA. This method seeks center wavelength and wavelength range of spectral sensitivity using training data to obtain the highest restoration accuracy. However, the filter arrangement of MSFA is fixed in this method. Hence, by changing the training data, spectral sensitivities are changed, but the number of the observation wavelength and filter arrangement are not changed. Shinoda et al.'s method [9] improves restoration accuracy by optimizing the filter arrangement under a given observation wavelength. However, the spectral sensitivities cannot be optimized. Conventional methods cannot optimize both the observation wavelengths and filter arrangement simultaneously based on the imaging object.

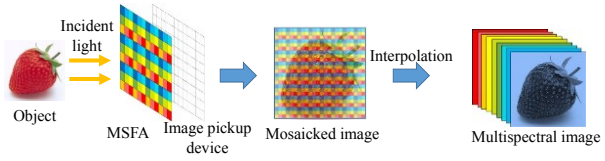

Figure 1. MSI imaging system flow using MSFA.

In this paper, we propose a method that optimizes the number of the observation wavelengths, each observation wavelength, and filter arrangement based on an imaging object. The proposed method designs MSFA using the full-resolution MSI of the assumed imaging object. The proposed method uses a full-resolution MSI as the training data and simulates mosaicking and interpolation on a computer. The optimal MSFA is designed to minimize the mean squared error (MSE) between MSI and restored MSI. The optimal MSFA is acquired by minimizing MSE based on simulated annealing (SA).

The rest of this paper is organized as follows: in Section 2, we describe our design method for MSFA. In Section 3, we discuss the experiment results. Section 4 presents our conclusions.

2. Optimizing method for MSFA using training data

In the proposed method, MSFA is optimized in order to minimize the mean squared error (MSE) between the training data and restored MSI. The training data is full-resolution X-band MSI that captures a specific object with a single-camera multi-shot system [2]. Figure 2 shows the process of creating the restored MSI for MSFA evaluation. In Figure 2, $W=\{f_1, f_2, \cdots, f_X\}$ is a set of observation wavelengths of the training data, where f_i denotes the i-th observation wavelength of the training data. $S=\{f_{d1}, f_{d2}, \cdots, f_{dN}\}$ is a subset of W, and N is the number of elements of S ($N \leq X$). To clearly specify the number of elements, S that consists of N elements is represented as S^N in this paper. P is the set of 2D positions $\{(x_1, y_1), (x_2, y_2), \ldots, (x_i, y_i), \ldots, (x_N, y_N)\}$ under a given S^N. Here, (x_i, y_i) represents the position of the i-th element of S^N in MSFA. P is regarded as the MSFA pattern. As shown in Figure 2, N-band MSI is created by downsampling in the wavelength domain based on S. Then, the mosaicked MSI is created based on P. Subsequently, N-band MSI is restored by interpolating the mosaicked MSI in the space domain, and X-band MSI is restored by interpolating the N-band MSI in the wavelength

DOI: 10.2352/ISSN.2470-1173.2016.15.IPAS-024

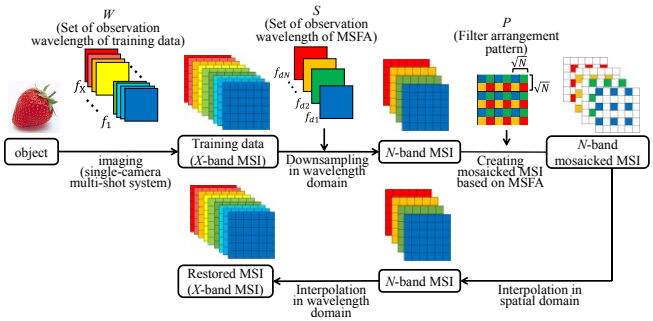

Figure 2. Flow to create restored MSI from training data for MSFA evaluation.

domain. In this paper, we apply Brauers' demosaicking [10] to restore *N*-band MSI, and Wiener estimation [13] to restore *X*-band MSI from *N*-band MSI. Here, the Wiener estimation matrix consists of the first-order Markov process with the correlation coefficient $\rho = 0.9995$[14].

In Figure 2, we assume that an optimal MSFA is not always an *X*-band MSFA, and explore an *N*-band MSFA ($N \le X$). If *X* is large, interpolation accuracy in the spatial domain becomes very low because the observation points of each band become very sparse. The restored accuracy depends on the sampling density in both the spatial and wavelength directions. Therefore, the optimal MSFA is not always an *X*-band MSFA for restoring an *X*-band MSI, and the flow of Figure 2 does not limit the number of bands of MSFA to *X*.

In the proposed method, the restored *X*-band MSI depends on three-elements, that is *N*, S^N, and *P*. If we examine all the patterns of *N*, S^N, and *P*, the optimal MSFA that minimizes MSE between the restored image and training data can be obtained. However, an optimizing process by brute force is not practical because the combination number of *N*, S^N, and *P* is vast. Hence, in the proposed method, although we use brute force to optimize the number of the observation wavelength *N*, the optimal set of observation wavelengths *S* and filter arrangement patterns *P* are obtained based on SA.

The proposed optimizing algorithm consists of three algorithms. Algorithm 1 acquires P_{opt1}, which is the MSFA constructed by optimizing *N*, S^N, and *P*. Algorithm 2 acquires P_{opt2}, which is the MSFA constructed by optimizing S^N and *P* under a given *N*. Algorithm 3 acquires P_{opt3}, which is the MSFA constructed by optimizing *P* under a given S^N.

The process for acquiring P_{opt1} is presented in Algorithm 1, where *T* is the *X*-band MSI used for training data. P_{opt1} is MSFA constructed by optimizing the three elements *N*, S^N, and *P*. First, the number of the observation wavelength *N* is initialized as $N \leftarrow i^2$. Because MSFA is constructed by a block arrangement whose size is $\sqrt{N} \times \sqrt{N}$, as shown in Figure 2, *N* is the square of the integer and $N \le X$. P_i is *N*-band MSFA optimized under a given *N*. P_i is acquired by using Algorithm 2. After obtaining all P_i from i=1 to $\sqrt{N}$, P_{opt1} is calculated by

$$P_{opt1} = \arg\min_{P_i \forall i} g(P_i, T), \quad (1)$$

where $g(P, T)$ is the function that calculates MSE between *T* and the demosaicked image with *P*.

The process for acquiring P_{opt2} is presented in Algorithm 2, where P_{opt2} is acquired based on input *T* and *N*. First, set S^N is created randomly by the chosen *N* elements from set *W*. $\bar{S}^N$ is the set of non-selected observation bands; namely, $\bar{S}^N$ is a complementary set of S^N. P_j^N is an optimized MSFA under a given S^N. P_j^N is acquired by Algorithm 3. After obtaining P_j^N, S^N is updated for the next iteration. S'^N is S^N, whose one element is swapped with one of $\bar{S}^N$ at random. Then, S^N is updated to S'^N according to probability q_1 determined by comparing MSE as follows:

Algorithm 1: Optimizing MSFA

Input: X-band MSI used for training data: *T*
Output: Optimized MSFA: P_{opt1}
Initialization:
Iteration counter: $i \leftarrow 1$
Number of bands: *N*
Repeat
$i \leftarrow i + 1$
$N \leftarrow i^2$
$P_i \leftarrow$ Algorithm 2(T, N)
Until $N > X$
Return $P_{opt1} = \arg\min_{P_i \forall i} g(P_i, T)$

Algorithm 2: Optimizing *N*-band MSFA

Input: *T*, *N*
Output: Optimized MSFA under a given *N*: P_{opt2}
Initialization:
Iteration counter: $j \leftarrow 1$
Random subset of *W*: S^N
Complement of S^N: $\bar{S}^N$
Optimized MSFA under a given *j*-th S^N: P_j^N
Repeat
$S'^N \leftarrow S^N$, whose one element is swapped with one of $\bar{S}^N$ at random.
$P_j^N \leftarrow$ Algorithm 3(S^N)
$P'^N_j \leftarrow$ Algorithm 3(S'^N)
S^N is updated to S'^N according to the probability of eq. (2).
$j \leftarrow j + 1$
Until j = 10000
Return $P_{opt2} = \arg\min_{P_j^N \forall j} g(P_j^N, T)$

Algorithm 3: Optimizing *N*-band MSFA under S^N

Input: S^N
Output: Optimized MSFA under a given S^N: P_{opt3}
Initialization:
Iteration counter: $k \leftarrow 1$
MSFA under a given S^N and *k*-th pattern: $P_k^{S^N}$
$P_1^{S^N}$ is random arrangement pattern under a given S^N.
Repeat
$k \leftarrow k + 1$
$P_k^{S^N} \leftarrow P_{k-1}^{S^N}$
$P'^{S^N}_k$ is created by swapping two elements of $P_k^{S^N}$ at random.
$P_k^{S^N}$ is updated to $P'^{S^N}_k$ according to the probability of eq. (4).
Until k=10000
Return $P_{opt3} = \arg\max_{P_k^{S^N} \forall k} h(P_k^{S^N})$

©2016 Society for Imaging Science and Technology
DOI: 10.2352/ISSN.2470-1173.2016.15.IPAS-024

$$q_1(\Delta_1, t_1) = \begin{cases} 1 & (\Delta_1 \geq 0) \\ e^{\frac{\Delta_1}{t_1}} & (\Delta_1 < 0) \end{cases} \quad (2)$$

$$\Delta_1 = g(P_j^N, T) - g(P'^N_j, T) \quad (3)$$

where t_1 is the temperature. The annealing schedule is repeated for $t_1 := 0.9993 \times t_1$, where t_1 is set to 10000 in the initialization, and the annealing schedule is terminated at 10,000 iterations. Finally, P_{opt2} that derives the minimum MSE from P_1^N to P_{10000}^N is returned.

The process for acquiring P_{opt3} is presented in Algorithm 3, which optimizes MSFA under a given S^N based on the interpolation quality metric (IQM) [9]. $h(P)$ is the IQM value calculated based on P. A higher $h(P)$ corresponds to higher demosaicking quality. In this algorithm, the optimal filter arrangement under a given S^N is derived by maximizing $h(P)$ using SA. $P_1^{S^N}$ is the random arrangement pattern under a given S^N. $P'^{S^N}_k$ is created by swapping two elements of $P_k^{S^N}$ at random, which means that two arbitrary MSFA filters are swapped. Then, $P_k^{S^N}$ is updated to $P'^{S^N}_k$ with probability q_2 determined by comparing IQM as follows:

$$q_2(\Delta_2, t_2) = \begin{cases} 1 & (\Delta_2 < 0) \\ e^{\frac{\Delta_2}{t_2}} & (\Delta_2 \geq 0) \end{cases} \quad (4)$$

$$\Delta_2 = h(P_k^{S^N}) - h(P'^{S^N}_k) \quad (5)$$

where t_2 is the temperature. The annealing schedule is repeated for $t_2 := 0.999 \cdot t_2$, where t_2 is set to one in the initialization, and the annealing schedule is terminated at 10,000 iterations. Finally, P_{opt3} that derives maximum IQM from $P_1^{S^N}$ to $P_{10000}^{S^N}$ is returned.

Algorithm 3 obtains the best MSFA under a given S^N. Algorithm 2 obtains the best MSFA under a given N by applying Algorithm 3 with changing S^N. In Algorithm 1, MSFAs are obtained by applying Algorithm 2 with changing N; finally, P_{opt1} is obtained as the best MSFA with optimized N, S^N, and P.

3. Experiment results

We show the validation of the proposed method through an experiment. In this experiment, we use three pathological MSIs. Figure 3 shows an sRGB image converted from these pathological MSIs captured at 20× magnification, 512×512 pixels, and 51 bands from 420 to 720 nm at 6 nm. The pathological tissue is of an H&E-stained liver (US Biomax, Hepatocellular Carcinoma Tissue Array C054). The imaging system uses an optical microscope (Olympus, BX53), liquid crystal tunable filters (CRi, Varispec VIS), and monochrome CCD (Point Grey,Grasshopper 3).

Normally, we should create optimized MSFA by using many pathological images. However, because we have no more than three sample images, that verification is difficult. Hence, in this paper, we regard each image as individual training data, and we create three optimized MSFAs. We examine the performance of the optimized MSFAs using training data as a test image. We evaluate the peak signal-to-noise ratio (PSNR) of each MSFA, and

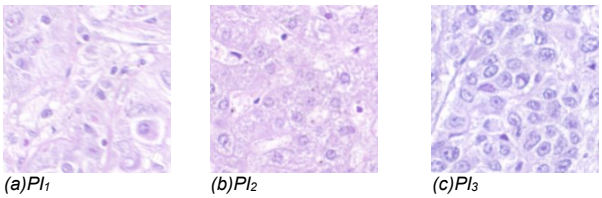

Figure 3. sRGB images converted from three pathological MSI.

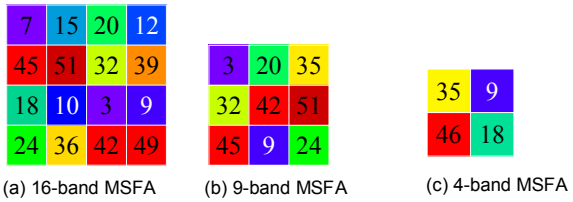

Figure 4. N-band MSFAs created by proposed method.

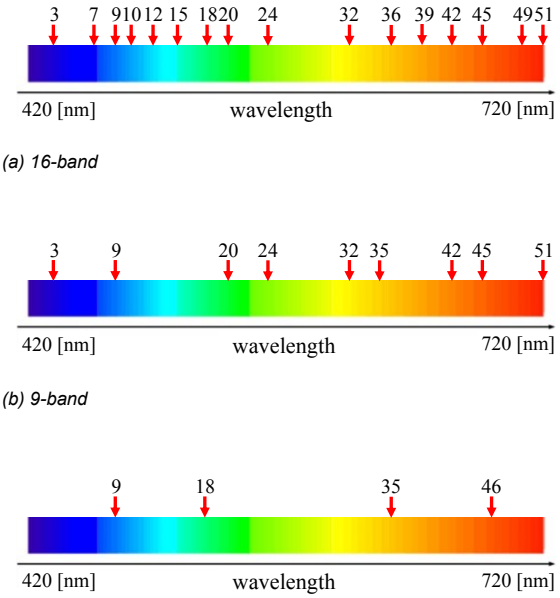

Figure 5. Observation wavelength for each MSFA.

Table 1. PSNR of the restored images at each MSFA.

	PI_1	PI_2	PI_3
16-band MSFA	31.196	31.372	31.324
9-band MSFA	31.584	31.650	31.739
4-band MSFA	30.094	29.336	30.386

consider the difference of each MSFA. Figure 4 shows MSFAs whose numbers for the observation wavelengths are 16, 9, and 4. These MSFAs are created by Algorithm 2 when N is 16, 9, and 4, and T is PI_1. From Figure 4, the closer bands in the wavelength

©2016 Society for Imaging Science and Technology
DOI: 10.2352/ISSN.2470-1173.2016.15.IPAS-024

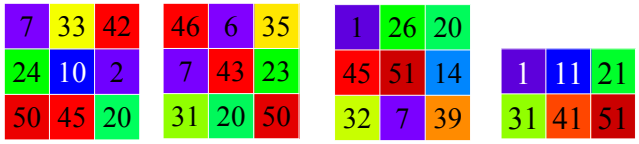

(a) Proposed for PI_2 (b) Proposed for PI_3 (c) Shinoda et al. (d) Brauers et al.

Figure 6. MSFA by each method.

Table 2. PSNR calculated by each method [dB].

	Proposed	Shinoda et al.	Brauers et al.
PI_1	31.584	30.988	28.499
PI_2	31.650	30.980	27.381
PI_3	31.739	31.230	28.131

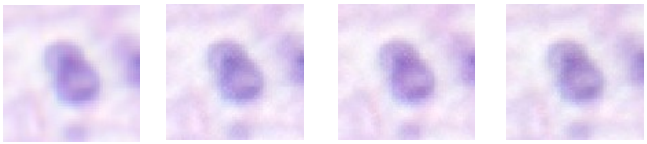

(a) Original image (b) Proposed (c) Shinoda et al. (d) Brauers et al.

Figure 7. Enlarged original and restored images for each method.

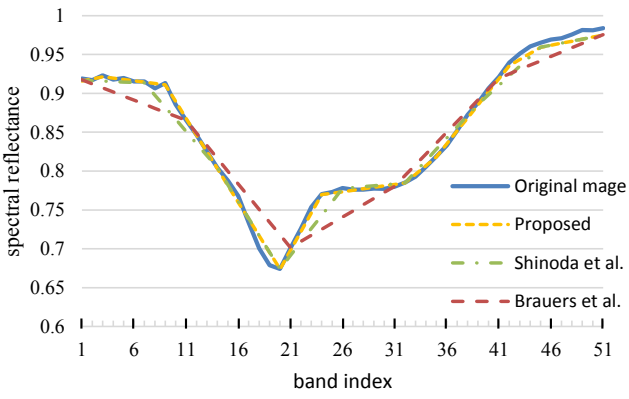

Figure 8. Spectrum comparison.

domain are comparatively distant from each other in the spatial domain. Figure 5 shows the chosen observation wavelength of each MSFA. Here, the numbers are the band indices named from short to long wavelengths in the 51-band MSI. As shown in Figure 5, the chosen N bands are not always at regular intervals, because the proposed method chooses bands in order to minimize MSE of the restored MSI. Table 1 indicates PSNR of the restored images at each MSFA. From Table 1, we can see that when the number of the observation band is nine, PSNR is the highest. Hence, the nine-band MSFA shown in Figure 4 (b) is the best MSFA for the recovering PI_1. Figure 6 (a) shows MSFAs created by the proposed method based on PI_2, in a similar way. Figure 6 (b) shows MSFA of PI_3. Because the number of the observation bands for PI_2 and PI_3 of MSFAs created by the proposed method is also nine, as indicated in Table 1, the best MSFA for capturing 51-band pathological images is the nine-band MSFA. If the number of the observation bands of MSFA is increased, interpolation processing in the spatial domain becomes difficult because the measuring density becomes sparse in each observation band. On the other hand, interpolation processing in the wavelength domain becomes easy, because the number of the observation wavelengths increases. Hence, interpolation accuracy of the spatial and wavelength domains is in a trade-off relationship. Therefore, even if the number of the observation wavelength is increased, the restoration accuracy is not always improved.

Table 3. Experiment environment.

OS	Windows 7 professional
Memory	8.00GB
Processor	Intel(R) Core(Tm) i7-4790 CPU 3.60GHz
Software	MATLAB 8.2.0

Table 4. Computational times [h].

	Computational time
Proposed	18.6111
Shinoda et al.	0.0003

Figure 6 (c) shows MSFA created by Shinoda et al.'s method, and Figure 6 (d) shows MSFA created by Brauers et al.'s method. In Shinoda et al.'s method, because the algorithm for determining the number of the observation wavelength is not contained, we set the number of the observation wavelength to nine-bands in common with the proposed method. In Brauers et al.'s method, the number of the observation wavelength is six. Moreover the observation wavelengths of these methods are chosen at regular intervals. From Figure 6, we can see that the closer bands in the wavelength domain are comparatively distant from each other in the spatial domain, as is the case with PI_1. Table 2 indicates the PSNR calculated based on MSFAs created by each method. As demonstrated in Table 2, PSNR of the proposed method is higher than that of the conventional methods for all images. This is because the proposed method considers the observation wavelength for MSFA in addition to the arranging filter. Figure 7 shows enlarged views of the restored images. We cannot confirm the great differences between each method through visual observation. Therefore we compare the average spectral of the entire image as shown in Figure 8. From Figure 8, we can see that in Shinoda et al.'s method, a large error is confirmed from the 8th to 13th band and from 21st to 25th band. In Brauers et al.'s method, the error is large overall. However, the error of the proposed method is smaller than that of the conventional methods at these points. This is because MSFA of the proposed method observe the wavelengths that are difficult to interpolate through wiener estimation. From the above results, effectiveness of the proposed method is confirmed.

We compare the computational time of optimizing 16-band MSFA by proposed method Algorithm2 and Shinoda et al.'s method. Table 3 shows the experiment environment, and Table 4 shows the computational times of each method. The computational time of proposed method requires a lot of time than Shinoda et

DOI: 10.2352/ISSN.2470-1173.2016.15.IPAS-024

al.'s method. This is because the proposed method optimizes not only the filter arrangement, but also the observation wavelengths. The long computational time is not a big problem, because this program is applied on the design stage of MSFA. However, the improvement of the algorithm and the reduction of computational time are considered as future works.

4. Conclusion

In this paper, we proposed an optimization method for MSFA using training data. Experiment results demonstrated that MSFA optimized by the proposed method improves restoration accuracy. In the future, we plan to design an MSFA whose observation wavelength number is not the square of an integer, and use more training data.

Acknowledgment

This work was supported by JSPS KAKENHI Grant Numbers 15K20899, Grant-in-Aid for Scientific Research on Innovative Areas (No. 26108002) and the Center for Optical Research and Education of Utsunomiya University.

References

[1] Y. Monno, M. Tanaka, M. Okutomi, "Multispectral Demosaicking Using Adaptive Kernel Upsampling," Proc. of IEEE International Conference on Image Processing (ICIP), pp.3218-3221, Sept. 2011.

[2] O. Khait, S. Smirnov, C.D. Tran, "Time-Resolved Multispectral Imaging Spectrometer," Appl. Spectrosc. vol. 54, pp.1734–1742, 2000.

[3] X. Lin, G. Wetzstein, Y. Liu, and Q. Dai, "Dual-Coded Compressive Hyper-Spectral Imaging," IIH-MSP., pp.607-610, Oct. 2010.

[4] A. Wagadarikar, N. P. Pitsianis, X. Sun, D. J. Brady, "Video Rate Spectral Imaging Using a Coded Aperture Snapshot Spectral Imager," Opt. Express, vol.17, pp.6368-6388, 2009.

[5] Y. Monno, M. Tanaka, M. Okutomi, "Direct spatio-spectral datacube reconstruction from raw data using a spatially adaptive spatio-spectral basis," Proc. SPIE, vol. 8660, Feb. 2013.

[6] L. Miao and H. Qi, "The Design and Evaluation of a Generic Method for Generating Mosaicked Multispectral Filter Arrays," IEEE Trans. Image Process., vol.15, no.9, pp.2780-2791, 2006.

[7] L. Miao, H. Qi, R.Ramanath, and W.E. Snyder, "Binary Tree-based Generic Demosaicking Algorithm for Multispectral Filter Arrays," IEEE Trans. Image Process., vol.15, no.11, pp.3550-3558, 2006.

[8] Y. Monno, T. Kitao, M. Tanaka and M. Okutomi, "Optimal Spectral Sensitivity Functions for a Single-Camera One-Shot Multispectral Imaging System," Proc. of IEEE ICIP, pp.2137-2140, Sept. 2012.

[9] K. Shinoda, T. Hamasaki, M. Hasegawa and S. Kato, "Quality Metric for Filter Arrangement in a Multispectral Filter Array," Picture Coding Symposium, pp.149-152, Dec. 2013.

[10] J. Brauers, and T. Aach, "A Color Filter Array based Multispectral Camera," Proc. of Workshop Farbbildverarbeitung, Oct. 2006.

[11] S. Kirkpatrick, C. D. Gelatt and M. P. Vecchi, "Optimization by Simulated Annealing," Science, Vol.220, No.4598, pp.671-680, May 1983.

[12] H. Fukuda, T. Uchiyama, H. Haneishi, M. Yamaguchi, and N. Ohyama, "Development of 16-bands multispectral image archiving system," Proc. of SPIE, vol. 5667, pp. 136–145, 2005.

[13] H. Haneishi, T. Hasegawa, A. Hosoi, Y. Yokoyama, N. Tsumura, and Y. Miyake, "System design for accurately estimating the spectral reflectance of art paintings," Applied Optics, vol. 39, no. 35, pp. 6621– 6632, 2000.

[14] Y. Murakami, M. Yamaguchi and N. Ohyama, "Piecewise Wiener estimation for reconstruction of spectral reflectance image by multipoint spectral measurements," Appl. Opt., vol. 48, pp. 2188–2202, 2009.

Author Biography

Yudai Yanagi received a B.E. degree from Utsunomiya University, Utsunomiya, Japan, in 2015. His current research interests include multispectral imaging.

Kazuma Shinoda received B.E. and M.E. degrees from Niigata University, Niigata, Japan, in 2005 and 2007, respectively, and his Ph.D. from Tokyo Institute of Technology, Yokohama, Japan, in 2011. He is currently an assistant professor in the Graduate School of Engineering, Utsunomiya University, Japan. His research interests include digital image processing, image compression, and multispectral imaging.

Madoka Hasegawa received B.E., M.E., and Ph.D. degrees in Engineering from Utsunomiya University, in 1994, 1996 and 1999, respectively. She is a professor in the Graduate School of Engineering, Utsunomiya University, Japan. Her current research interests include image coding, image processing, digital watermark and graphical passwords. She is a member of IEICE, ITE, IPSJ and IEEE.

Shigeo Kato received a B.S. in Engineering from Hokkaido University and D.E. degrees in Engineering from Tokyo University, Japan, in 1972 and 1989, respectively. He is a professor in the Graduate School of Engineering, Utsunomiya University, Japan. His current research interests include image coding, information theory, image processing and digital watermark. He is a member of IEICE, ITE, and IEEE.

Masahiro Ishikawa received a Ph.D. degree from Niigata University, Niigata, Japan, in 2006. He is currently an Assistant Professor with the Saitama Medical University. His current research interests include image processing and computer-aided diagnosis.

Hideki Komagata received B.E., M.E., and Ph.D. degrees in Information Engineering from Niigata University, Niigata, Japan, in 2003, 2005 and 2010, respectively. He is currently an assistant professor at the School of Biomedical Engineering, Saitama Medical University, Japan. His research interests include computer vision, and medical imaging.

Naoki Kobayashi received B.Sc. and M.E. degrees from Tokyo Institute of Technology, Tokyo, Japan, in 1979 and 1981, respectively, and a Ph.D. from Niigata University, Niigata, Japan, in 2000. He has been a professor in the School of Biomedical Engineering, Faculty of Health and Medical Care of Saitama Medical University since 2008. His research interests include image processing, image compression and bio-signal processing.